Phase Behavior of Poly(ethylene–1-butene) in Subcritical and Supercritical Propane: Ethyl Branches Reduce Segment Energy and Enhance Miscibility

Shean-jer Chen, Michal Banaszak, and Maciej Radosz*

Exxon Research and Engineering Company, Annandale, New Jersey 08801

Received June 8, 1994; Revised Manuscript Received August 15, 1994[⊗]

ABSTRACT: On the basis of experimental batch-cell data, increasing short-chain branch density is found to reduce the cloud-point pressure of poly(ethylene–1-butene) solutions in propane, by as much as a factor of 3. This trend is captured by a SAFT approximation via an effective segment energy that depends on the branch density. Increasing branch density is found to decrease the effective segment energy and, hence, to make it closer to that of propane, which is consistent with the enhanced miscibility of branchy poly(ethylene–1-butenes) in propane.

Introduction

Polyolefins are known to be completely miscible when pressurized with small olefins and alkanes, supercritical and subcritical. Phase transitions in such systems can be tuned with density and hence with pressure, temperature, and composition. Patterns and types of phase transitions in polyolefin systems, for example, lower critical solution temperature (LCST), upper critical solution temperature (UCST), U-LCST, vapor liquid (VL), and VLL, depend on the degree of asymmetry between the polymer and the solvent, as reviewed by Folie and Radosz.[1] For example, on the basis of experimental data for well-defined, nearly monodisperse model systems, systematic patterns of LCST, UCST, and U-LCST transitions were attributed to differences in molecular weight (between the polymer and the solvent) for alternating poly(ethylene–propylene)[2,3] and to differences in polarity and association for polyisobutylene.[4,5]

It is not well understood, however, how differences in branchiness and microstructure affect the patterns of polyolefin phase behavior in small hydrocarbons. Charlet and Delmas[6] and Charlet et al.[7] measured the lower critical end points (LCEP), that is, the LCST points in the presence of the solvent vapor, for a series of polymers, including ethylene–propylene copolymers differing in ethylene concentration (hence in methyl branch density), all the way from polyethylene through polypropylene, in C_5 to C_9 alkanes. They found that, for a given solvent, such as *n*-pentane, the LCEP temperatures increase with decreasing ethylene concentration and hence with increasing methyl branch density. In other words, the polypropylene LCEP (e.g., 422 K) is much higher than that for polyethylene (e.g., 353 K), which means that polypropylene is easier to dissolve in *n*-pentane than polyethylene is. Charlet and Delmas attributed this effect to correlations of molecular orientation (CMO) that stem from alignment and interactions of straight-chain ($-CH_2CH_2-$) sequences. A similar short-chain branchiness effect, of lowering the cloud-point temperatures, was found by Kleintjens et al.[8] for polyethylene in diphenyl ether and analyzed in the framework of lattice theory. More recently, Lohse et al.[9] determined Flory's χ parameters from the neutron scattering data for a series of poly(ethylene–1-butene) (EB) blends, and found that the values of χ were significantly dependent on the EB microstructure.

Our goal is to explore the extent to which the EB microstructure, characterized by the ethylene concentration and ethyl branch density, affects the EB phase behavior in a small, subcritical and supercritical, alkane, such as propane. Our approach is to measure high-pressure cloud-point transitions at constant composition in an optical batch cell and to model the experimental data on the basis of the statistical associating fluid theory (SAFT).

Experimental Section

Phase boundaries are measured in a batch optical cell equipped with a sapphire window, which makes it possible to observe phase transitions visually, and with a movable piston, which makes it possible to adjust pressure at constant composition. The maximum volume is 17 cm^3. Phase transitions are observed visually at constant temperature, typically in the form of cloud-point (dew-point or bubble-point type) transitions, by displaying the window image, via a borescope, on a video screen. A detailed description of the equipment and procedure for binary systems is provided by Chen and Radosz.[2]

In a few cases, we also report the lower critical end points (LCEP) measured independently in a glass tube experiment. Unless stated otherwise, the phase transitions are measured for solutions containing about 5 wt % polymer and are dew-point like; that is, the polymer-rich phase is the minor phase at the onset of phase separation.

The poly(ethylene–1-butene) samples used in this work have been prepared by hydrogenating polybutadiene. Polybutadiene, in turn, has been synthesized anionically (by Lewis Fetters) to minimize polydispersity (less than 1.1) and to control 1,2 addition by controlling the reaction medium polarity; the higher the polarity, the higher the 1,2 addition.[10] The level of 1,2 addition varies from sample to sample but is constant for a given sample. A generic structure of EB samples is shown below.

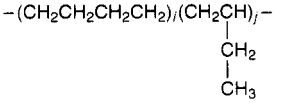

For each EB sample, there are *j* 1,2 units, and hence *j* ethyl branches, and *i* 1,4 units. The sequence of 1,2 units is random but uniform.

The properties of EB samples used in this work are given in Table 1. The polydispersity index, M_w/M_n, for the EB samples is less than 1.1, except for EB0, where it is 1.2. Also

* To whom correspondence should be addressed.

[⊗] Abstract published in *Advance ACS Abstracts,* January 15, 1995.

0024-9297/95/2228-1812$09.00/0

Table 1. Model Polymer Samples

sample code	branch density	mol % 1,2 units	wt % ethylene	$M_w \times 10^{-3}$	
EB0	0	0	100	120	NBS 1484 (data from Condo et al.[14])
EB4	4	8	92	62	$T_m = 114$ °C
EB19	19	32	68	96	$T_m = 41$ °C
EB35	35	52	48	85	$T_g = -61$ °C
EB79	79	88	12	91	$T_g = -34$ °C
EB94	94	97	3	90	$T_g = -22$ °C
PEP96K	50		40	96	alternating poly(ethylene−propylene)
EP130K	22		70	130	random, $M_w/M_n = 2$, $T_m = 40$ °C
PP210K	100		0	210	isotactic, $M_w/M_n = 2.2$, $T_m = 160$ °C

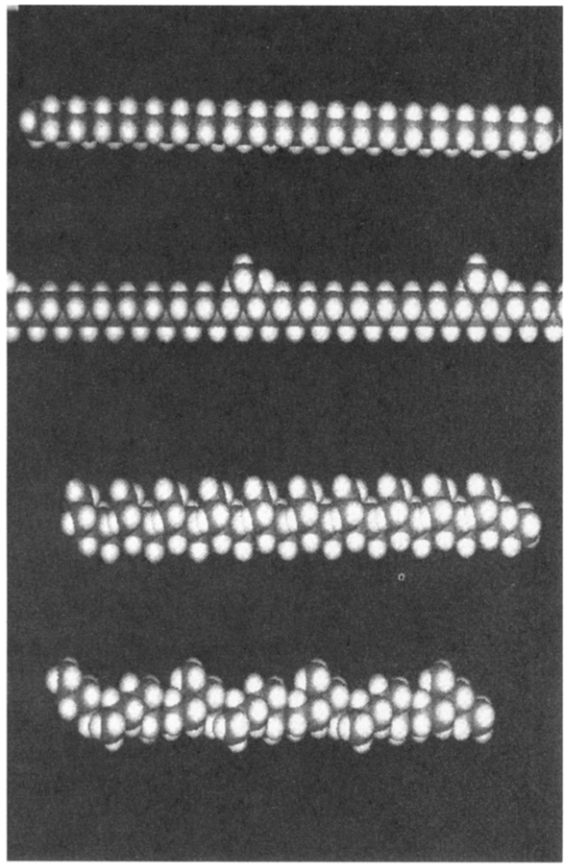

Figure 1. Space-filling examples of polyolefins with short-chain branches (M. Rabeony): (a) polyethylene backbone (EB0) with no side branches, (b) poly(ethylene−1-butene) with 20 ethyl branches per 100 backbone ethyls (EB20), (c) EB50, (d) alternating poly(ethylene−propylene), i.e., with 50 methyl branches per 100 backbone ethyls.

given in Table 1 are properties of an alternating poly(ethylene−propylene), PEP96K, a random poly(ethylene−propylene), EP130K, and an isotactic polypropylene, PP210K, which are also used in this work for comparison with the EB model systems. Branch density in Table 1, derived from NMR characterization, is the number of branches (ethyl for EB's, methyl for PEP, EP, and PP) per 100 ethyl units in the backbone. For EB's (but not for other comonomers, such as hexene and octene) the branch density is equal to the mol % 1-butene (on an ethylene + 1-butene basis). Branch density divided by 2 is equal to the number of branches per 100 carbons in the backbone (NMR reports usually give the number of branches per 1000 carbons in the backbone). The mol % 1,2 units (refers to 1,2 addition) is on the basis of counting straight chain C_4 units (two ethyl units) and branchy C_4 units (1-butene units); for EB's, the mol % 1,2 units is equal to the weight percent butene.

An example of space-filling models of EB's with three different branch densities (0, 20, and 50) and, for comparison, of an alternating poly(ethylene−propylene) is shown in Figure 1.

SAFT Model

SAFT is an acronym for an equation of state developed on the basis of the statistical associating fluid theory.[11,12] SAFT explicitly accounts for nonspecific (e.g., repulsive, dispersion) and specific (e.g., association due to hydrogen bonding) interactions among molecules and segments. In a simplified physical picture, a pure SAFT fluid is a collection of equisized hard-spherical segments that not only are exposed to mean-field (dispersion) forces but also (a) can be covalently bonded to form chain molecules and (b) can be weakly bonded to form short-lived clusters. Both covalent and hydrogen bond energies are modeled with square-well potentials.

The residual Helmholtz energy for a SAFT fluid, a^{res}, per mole of molecules, consists of four terms; hard-sphere (hs), chain, association (assoc), and dispersion (disp).

$$a^{res} = a^{hs} + a^{chain} + a^{assoc} + a^{disp} \tag{1}$$

Since the systems examined in this work do not exhibit specific interactions that can lead to association, we set a^{assoc} in eq 1 equal to zero. The hard-sphere and chain terms are calculated for pure components and extended to mixtures rigorously on the basis of statistical mechanics. The chain term depends on the number of segments per chain, m, and on the contact value of the radial distribution function of the reference fluid (hard sphere in this case), g^{hs}, as follows:

$$a^{chain}/RT = (1 - m) \ln g^{hs} \tag{2}$$

The dispersion term, however, requires mixing rules in order to be extended to mixtures. Detailed expressions for all the terms in eq 1, and the mixing rules (vdW1 used in this work), are described by Huang and Radosz.[11,12]

In order to calculate phase equilibria, e.g., the cloud points measured in this work, we need not only the detailed expressions for eq 1 but also values of three molecular parameters; segment number (m, number of segments per molecule), segment volume (v^{00}, in mL/mol of segments), and segment energy (u^0/k in kelvin, where k is the Boltzmann constant). We usually need the value of one binary parameter used in the mixing rule for the segment energy, which is either fitted to experimental data or estimated from empirical correlations.

The values of v^{00} and u^0/k, for the same class of compounds, are estimated to be constant for high molecular weights, e.g., $v^{00} = 12$ mL/mol and $u^0/k = 210$ K for the normal-alkane type compounds. The values of m are estimated from an empirical correlation developed for a series of alkanes[11,12]

$$m = 0.05096 M_w \tag{3}$$

Even though our model polymers have ethyl branches attached to the backbone, we approximate them as effective homopolymers, which is common to all the conventional equations of state for polymer systems. An example of such an approximation is application of the lattice cluster theory to EB copolymers by Banaszak et al.[13] Furthermore, somewhat arbitrarily, we set v^{00} equal to 12 mL/mol and estimate m from eq 3, same as for alkanes. However, we allow the u^0/k to vary with branch density.

We estimate an effective u^0/k in the spirit of the group contribution approaches. Specifically, we apply the van der Waals one-fluid mixing rule to estimate the average segment energy u^0/k for each EB separately, $(u^0/k)_{EB}$, as follows:

$$(u^0/k)_{EB} = x_E^2(u^0/k)_{EE} + 2x_E(1 - x_E)[(u^0/k)_{EE}(u^0/k)_{BB}]^{0.5} + (1 - x_E)^2(u^0/k)_{BB} \quad (4)$$

where x are the number fractions of segments, and u^0/k are the segment energies, in the polyethylene backbone (with subscript E) and in the ethyl branches (with subscript B). For example,

$$x_E = n_E/(n_E + n_B) \quad (5)$$

$$x_B = n_B/(n_E + n_B) \quad (6)$$

where n_E is the total number of backbone segments and n_B is the total number of branch segments, per molecule. The x_E and x_B are normalized in such a way that $x_E + x_B = 1$. Hence,

$$x_B = 1 - x_E \quad (7)$$

On the basis of the molecular weight M_w (weight average) and the branch density x_b (number of branches per 100 ethyl units in the backbone, which we derive from NMR), we can derive the number of carbons in the backbone (C_E) and in the branches (C_B). Since the number of segments is proportional to the number of carbons C, we can write

$$x_E = C_E/(C_E + C_B) \quad (8)$$

The C_B is related to C_E and x_b as follows:

$$C_B = \frac{x_b}{100}\frac{C_b}{2}C_E \quad (9)$$

where, in contrast to C_B, C_b is the number of carbons in a single branch. Since C_b is equal to 2 for EB's, the total number of carbons in the branches (per molecule) $C_B = (x_b/100)C_E$. In other words, substituting C_B into eq 8,

$$x_E = \frac{1}{1 + \frac{x_b}{100}} \quad (10)$$

We note that x_b is the branch density that is different from x_B, which is the number fraction of segments in the branches and is defined in eq 6.

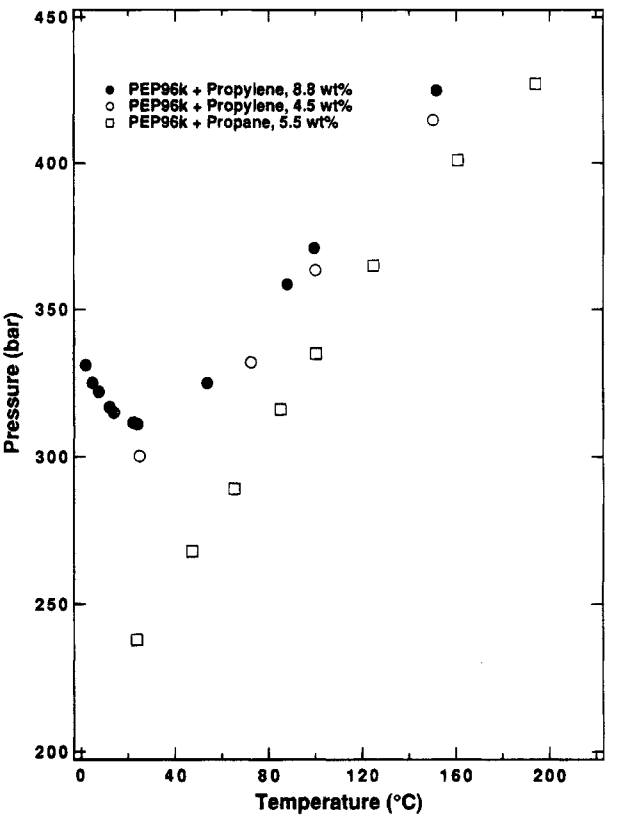

Figure 2. Pressure–temperature cloud points for propylene + PEP96K and propane + PEP96K which illustrate a weak polymer concentration effect in the 5–9 wt % range and a difference between propane and propylene. Propane is a slightly better solvent.

In order to calculate $(u^0/k)_{EB}$ from eq 4, we have to estimate $(u^0/k)_{EE}$ and $(u^0/k)_{BB}$, which is explained in the next section.

Results and Discussion

In an effort to relate the phase behavior of EB's in propane to that of PEP's in propylene, characterized in our earlier work,[2] we compare the effect of replacing propylene by propane. The experimental results, in the form of cloud-point pressures plotted versus temperature, are shown in Figure 2 for PEP96K in 5.5 wt % propane (squares) and, separately, for PEP96K in 4.5 (circles) and in 8.8 (triangles) wt % propylene. All the cloud-point transitions shown in Figure 2, and in all the other figures in this work, are measured in the batch cell and are of the dew-point type. Figure 2 supports two observations.

First, the cloud-point pressures for propane are systematically lower than those for propylene by about 20–30 bar. This means that, compared to propane, propylene is a weaker solvent for PEP, which can be explained by its dipolarity and lower density. Second, the effect of propylene composition in the range of around 5–10 wt % is relatively small, at least for higher molecular weight polyolefins, such as PEP96K.

Next, we compare the effect of replacing PEP96 by a corresponding EB (e.g., EB35), both in propane. This is shown in Figure 3. EB35 requires higher pressures to become completely miscible with propane. This means that PEP96K is easier to dissolve in propane than EB35, in spite of having a somewhat higher molecular weight than EB35. This is noteworthy because, within the same group of polyolefins (e.g., PEP's),[2] the cloud-point pressure increases with increasing molecular weight. Therefore, it must be the difference in

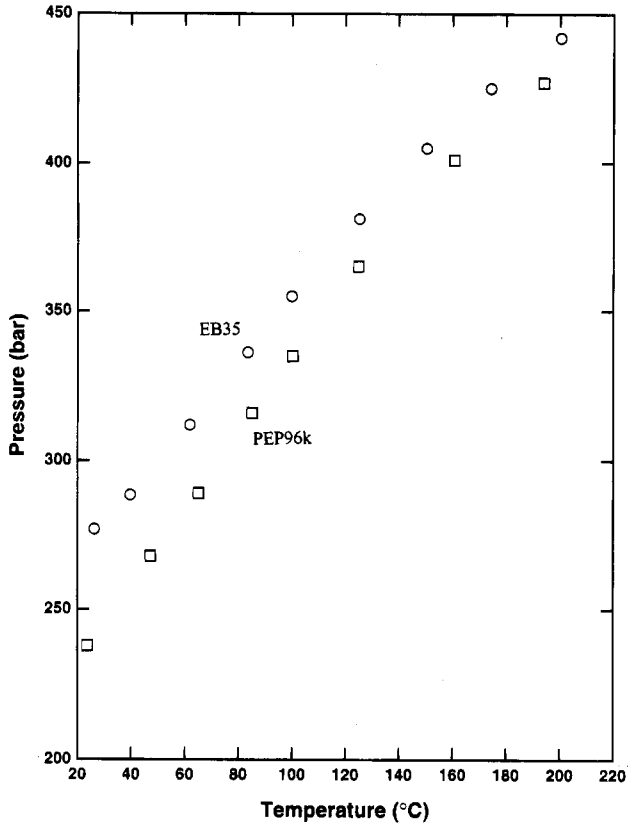

Figure 3. Pressure–temperature cloud points for propane + PEP96K (alternating methyl branches and 48 wt % ethylene) and propane + EB35 (random ethyl branches and 40 wt % ethylene); example illustrating the ethylene weight percent effect for different branches and different branch distributions (alternating versus random).

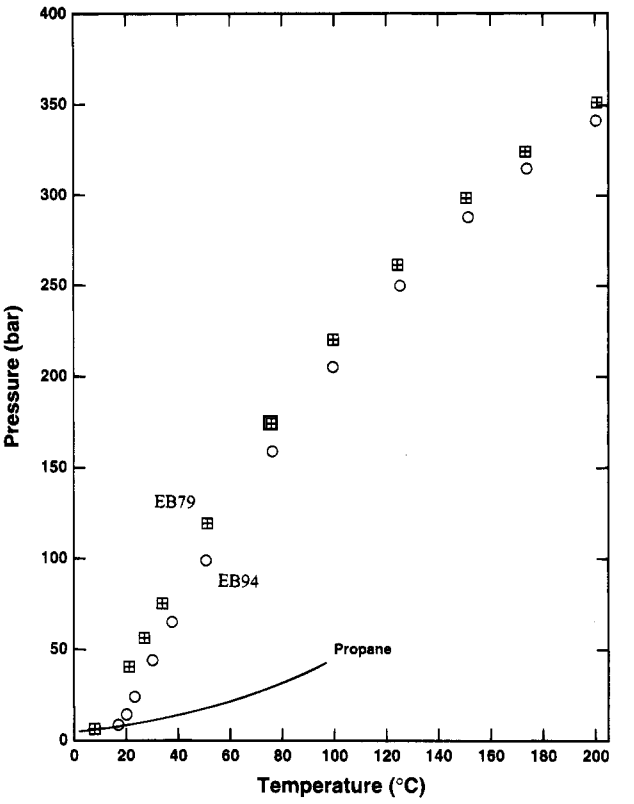

Figure 4. Pressure–temperature cloud points for propane + EB79 and propane + EB94 which illustrate the effect of ethyl-branch density.

microstructure that causes EB35 to have higher cloud point pressures, which one observes in Figure 3. The EB35 microstructure is different from that of PEP96K in two ways. One, EB35 has a higher ethylene weight percent (48 versus 40, on the basis of Table 1) and a lower branch density (35 versus 50). Two, the side branches on EB35 are randomly distributed ethyl branches, whereas those on PEP96K are alternating methyl branches. Let us focus on the effect of branch density.

In order to explore the effect of branch density, we compare two EB's having nearly identical molecular weights (91 000 and 90 000) but slightly different branch densities, EB79 and EB94, both in propane. As it is shown in Figure 4, both EB's exhibit a LCST type behavior but EB94 has lower cloud-point pressures. The difference is not large (on the order of 10 bar), but it is systematic. This observation means that increasing the branch density decreases the cloud-point pressure; it shifts the cloud-point curve to lower pressures. For the record, the LCEP points (where the LCST curve intersects the propane vapor pressure curve in the *PT* projection) measured in a separate glass-tube experiment are consistent with the LCST points measured in the batch cell.

A more complete illustration of the branch density effect is shown for other EB's in Figure 5. The upper cloud-point-pressure limit is set by experimental data points[14] for a linear polyethylene (EB0), with no side branches. Except for the one point at the lowest temperature (above 700 bar) that represents a solid–liquid transition, the other points for EB0 are of the fluid–liquid type, and they fall on a U-LCST curve. The lower cloud-point-pressure limit is set by the LCST curve for EB94. On the basis of the experimental data shown in Figure 5, one observes that increasing the branch density not only decreases the cloud point pressures, by as much as a factor of 3 but also shifts the phase behavior type, from U-LCST to LCST for high branch densities.

The reduction of the cloud-point pressures (as results with increasing the branch density) corresponds to an increase in the LCEP temperatures for the LCST which is explained by Charlet and Delmas[6] in terms of a short-range correlation of molecular orientation (CMO). The probability of CMO increases as the concentration of polyethylene sequences (those with no side branches) increases. In other words, high ethylene content, as well as nonuniform distribution of branches (e.g., random or blocky, rather than alternating), is likely to induce high degrees of CMO. Our data are consistent with this explanation, as it is shown in Figure 6, where the cloud-point pressure is plotted versus mass percent ethylene in polyolefin. While not free from scatter, the experimental points in Figure 6 suggest a monotonic increase in the cloud pressure upon increasing the ethylene content and decreasing the branch density.

While increasing the ethylene content often (but not always) increases the degree of crystallinity, it turns out that the cloud-point pressures are not well correlated to the degree of crystallinity and melting point. For example, we compare two commercial polyolefins, poly(ethylene–propylene), EP130K with T_m = 40 °C, and isotactic polypropylene, PP210K with T_m = 160 °C. Their experimental *PT* phase diagram is shown in Figure 7. The PP210K system exhibits a solid–liquid transition around 120 °C. However, its cloud-point pressures are well below those for EP130K, even though its melting point and molecular weight are much higher. Therefore, we attribute these lower cloud-point pres-

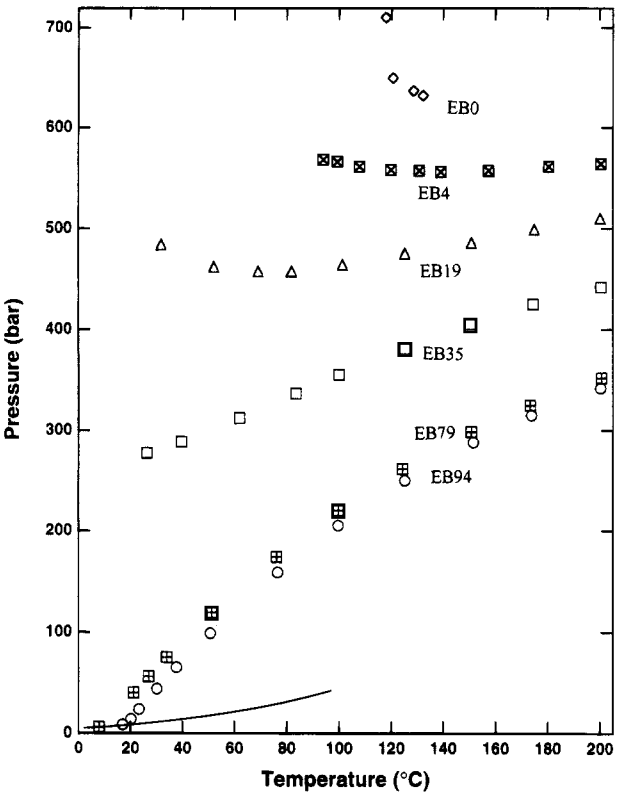

Figure 5. Pressure–temperature cloud points for propane + EB0 through EB94. Increasing the ethyl branch density not only lowers the cloud-point pressure (by as much as a factor of three) but also shifts the phase behavior type from U-LCST to LCST. The point for EB0 above 700 bar is of the solid–liquid type. All other points are of the liquid–liquid, dew-point-like type.

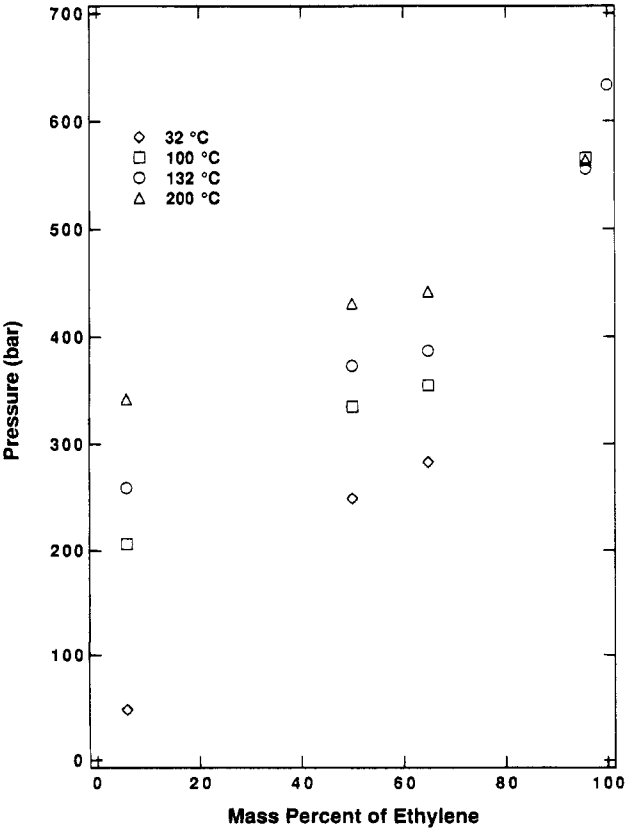

Figure 6. Cloud-point pressures for propane + EB0 through EB94 plotted versus mass percent of ethylene in polymer.

sures for PP210K to its low ethylene content (zero) and much higher branch density (100 versus 22 for EP130K).

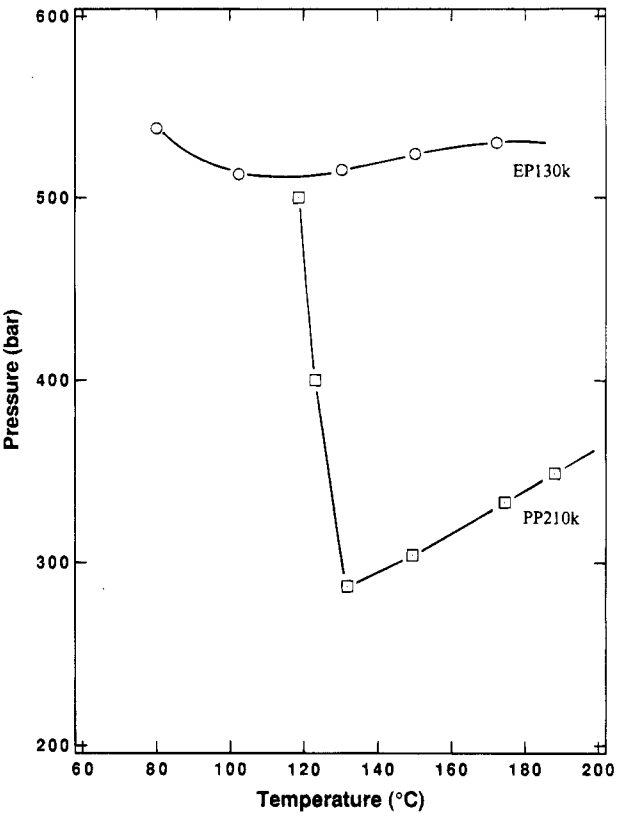

Figure 7. Pressure–temperature cloud points for propane + EP130K (10.2 wt %, circles) and propane + PP210K (3.3 wt %, squares). At temperatures above the solid–liquid line for PP210K (around 130 °C), the polypropylene cloud-point pressures are much lower than those for EP130K.

Table 2. SAFT Parameters for EB + Propane[a]

	u^0/k, K	v^{00}, mL/mol	m
E	210	12	
B	170	12	
EB	eq 4	12	$0.05096M_w$
propane	193	13.46	2.7

[a] E designates segments in the polyethylene backbone; B designates segments in branches (ethyl branches formed by 1-butene units); EB designates the EB copolymer.

Table 3. Example of Effective Segment Energies Estimated for EB's

sample	$(u^0/k)_{EB}$, K
EB0	210
EB19	203
EB94	190

These trends are reproduced qualitatively with SAFT. The approach is to fit one binary parameter (k_{ij}, used in the mixing rule for the segment energy) to the data points for EB0. This binary parameter is then treated as a universal constant, independent of temperature and branch density. Since we approximate the branchy EB's as effective homopolymers, we find that we can capture the effect of variable branch density using effective segment energies estimated from eq 4. The only parameter that has to be fitted to experimental data is the segment energy for the branches, $(u^0/k)_{BB}$ in eq 4. We estimate $(u^0/k)_{BB}$ to be around 170 K (Table 2) on the basis of a data point for EB94 only, without attempting to optimize it at this stage. Next, we estimate $(u^0/k)_{EB}$ for other EB's from eq 4. Examples are given in Table 3. We find that the effective segment energy $(u^0/k)_{EB}$ decreases with increasing branch density. This is reassuring because the segment energies of branchy EB's, which are more readily miscible with

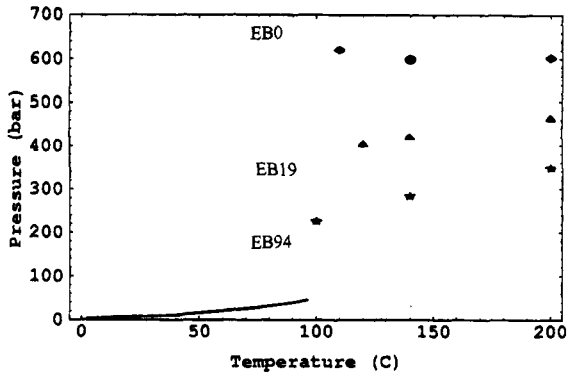

Figure 8. Pressure–temperature cloud points for propane + EB0, + EB19, + EB94. Estimated from SAFT.

propane, are closer to the segment energy of propane (193 K, Table 2) than that of EB0. In other words, the branchy EB's and propane are more alike than polyethylene and propane.

The results of SAFT calculations are shown in Figure 8 for two extreme cases, EB0 and EB94, and for one intermediate case, EB19. SAFT captures the factor of 3 difference in the cloud-point pressure in going from EB0 to EB94. SAFT also captures the shift from U-LCST to LCST.

Conclusions

Increasing short-chain branch density is found to reduce the cloud-point pressure of poly(ethylene–1-butene) solutions in propane, by as much as a factor of 3. This means that short-chain branchiness enhances miscibility with propane. This trend is captured by the homopolymer SAFT approximation via an effective segment energy that depends on the branch density. Increasing branch density is found to decrease the effective segment energy and, hence, to make it closer to that of propane, which is consistent with the enhanced miscibility of branchy EB's in propane.

Acknowledgment. A preliminary account of this work was presented during the Annual Meeting of AIChE in St. Louis in 1993. We are grateful to L. J. Fetters, J. Sissano, D. J. Lohse, and W. W. Graessley for sharing with us their EB samples, to D. J. Lohse for sharing with us unpublished data for EB blends, and to M. Rabeony for preparing Figure 1.

Supplementary Material Available: Tabulated experimental data taken in this work for EB's, including cloud-point data obtained in a high-pressure batch cell and LCEP (lower-critical end point) data obtained in a glass tube (1 page). Ordering information is given on any current masthead page.

References and Notes

(1) Folie, B.; Radosz, M. Phase Equilibria in High-Pressure Polyethylene Technology. *Ind. Eng. Chem. Res.*, in press.
(2) Chen, S. J.; Radosz, M. *Macromolecules* **1992**, *25*, 3089.
(3) Chen, S. J.; Economou, I. G.; Radosz, M. *Macromolecules* **1992**, *25*, 4987.
(4) Gregg, C. J.; Stein, F. P.; Radosz, M. Phase Behavior of Telechelic Polyisobutylene in Subcritical and Supercritical Fluids. 1. *Macromolecules* **1994**, *27*, 4972.
(5) Gregg, C. J.; Stein, F. P.; Radosz, M. Phase Behavior of Telechelic Polyisobutylene in Subcritical and Supercritical Fluids. 2. *Macromolecules* **1994**, *27*, 4981.
(6) Charlet, G.; Delmas, G. *Polymer* **1981**, *22*, 1181.
(7) Charlet, G.; Ducasse, R.; Delmas, G. *Polymer* **1981**, *22*, 1190.
(8) Kleintjens, L. A.; Koningsveld, R.; Gordon, M. *Macromolecules* **1980**, *13*, 303.
(9) Lohse, D. J.; Balsara, N. P.; Fetters, L. J.; Schulz, D. N.; Graessley, W. W.; Krishnamoorti, R. In *New Advances in Polyolefins*; Chung, T. C., Ed.; Plenum Press: New York, 1993; p 175 (and references thereof).
(10) Morton, M.; Fetters, L. J. *Rubber Rev.* **1975**, *48*, 359.
(11) Huang, S. H.; Radosz, M. *Ind. Eng. Chem. Res.* **1990**, *29*, 2284.
(12) Huang, S. H.; Radosz, M. *Ind. Eng. Chem. Res.* **1991**, *20*, 1994.
(13) Banaszak, M.; Petsche, I. B.; Radosz, M. *Macromolecules* **1993**, *26*, 391.
(14) Condo, P. D., Jr.; Colman, E. J.; Ehrlich, P. *Macromolecules* **1992**, *25*, 750.

MA941192J